2022

Generalized Disjunctive Programming-based, Mixed Integer Linear MPC Formulation for Optimal Operation of a District Energy System for PV Self-consumption and Grid Decarbonization: Field Implementation

Donghun Kim

Tianzhen Hong

Mary Ann Piette

Generalized Disjunctive Programming-based, Mixed Integer Linear MPC Formulation for Optimal Operation of a District Energy System for PV Self-consumption and Grid Decarbonization: Field Implementation

Donghun Kim[1*], Tianzhen Hong[1], Mary Ann Piette[1]

[1] Building Technology & Urban Systems Division,
Lawrence Berkeley National Laboratory, Berkeley, California, United States of America
Contact Information: donghunkim@lbl.gov

* Corresponding Author

ABSTRACT

Thermal energy storage (TES) for a cooling plant serving a campus or district of buildings can shift cooling energy from peak to non-peak hours so that it is able to reduce electrical operation costs in buildings and increase stability and operational efficiency in the grid. Traditionally, heuristic control approaches, such as the storage priority control, have been widely used in practice. Those simple control approaches have shown reasonable or even near-optimal performance in the past. However, the increasing penetration of renewables changes the situation: exposing the electrical grid to the growing supply demand challenge which encourages greater consumption at times when renewable energy is plentiful and lesser when dirtier supply is used. This paper presents a model predictive control (MPC) strategy, site demonstration and evaluation results for optimal operation of a chiller plant, TES and behind-meter photovoltaics for a campus-level district cooling system. The MPC was formulated as a mixed-integer linear program using the Generalized Disjunctive Programming for better numerical and control properties. Results show that the MPC can effectively utilize PV generated electricity to drive chillers for charging the TES during the day and avoid sending excess electricity back to the grid. Compared with the storage priority control, the MPC reduces the excess PV power by around 25%, the greenhouse gas emission by 10%, and peak electricity demand by 10%.

1. INTRODUCTION

Traditional control strategies for TES cooling plants, i.e., the storage priority or chiller priority controls, fully charge TES using chillers during OFF peak price period (typically a night time period) while discharging TES to meet cooling load partially or fully during ON peak price period (typically a day time period). Although the rule-based controls have shown near-optimal behavior and provided benefits to facilities, buildings, and the grid in the past by lowering the total electrical load during peak price period and hence requiring less spinning/non-spinning reserves and other back-up power plants in the grid, the rapid penetration of renewable energy resources is changing the situation. The intermittent nature of behind-meter renewable energy sources and the grid's movement toward more dynamic price signals challenge building or facility operators to rely on the rule-based operations.

Despite many studies of optimal operation of TES with behind-meter renewable and energy storages, a majority of them are using simulations as shown in the table, and therefore real performance of MPC including self-consumption ratio are not clear. Although there are some papers with experimental assessment of MPCs coordinating TES and HVAC systems, they are limited to small-scale systems, e.g., laboratory or small-sized building (e.g., residential) levels. For large-scale systems, there are very few papers that demonstrate an MPC for renewable energy integration and present site performance. In addition, there is a lack of knowledge about applying MPC to mitigate CO2 emissions (Tarragona et al., 2021).

This paper fills the gaps by implementing an MPC for a campus-level cooling TES plant and presenting on-site performance compared with carefully selected, historical rule-based operation data for the plant. The MPC aims at promoting the self-consumption of the on-site renewable and minimizing CO2 in the grid. Because utility cost reduction is one of the key motivations for the facility, the MPC is also formulated to reduce peak demand. In this paper, we present a novel MPC formulation (Mixed Integer Linear form using the Generalized Disjunctive Programming) and the site performance evaluation.

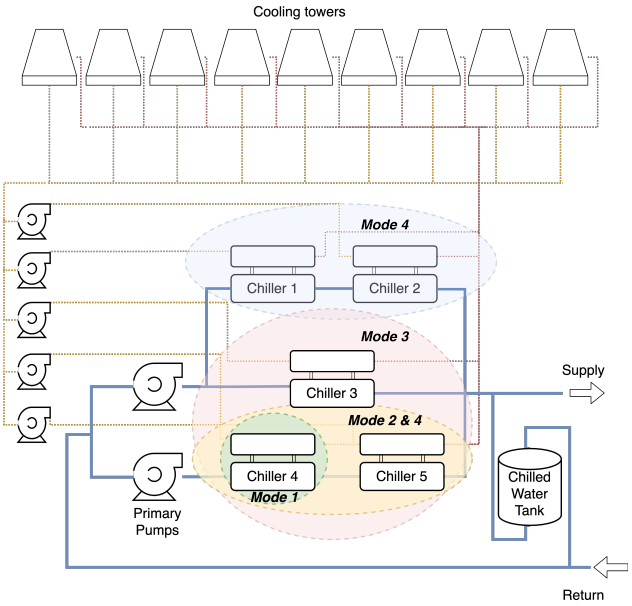

Figure 1: The equipment configuration of the central cooling plant at University of California, Merced

2. SITE DESCRIPTION AND BASELINE CONTROL STRATEGY

2.1 Site description

The central plant of the University of California, Merced is the demonstration site located in California, U.S. The cooling TES plant, shown in Fig. 1, has five chillers with a total cooling capacity of 17.6 MW, 5000 ton of refrigeration, serving around 40 buildings. It has the primary-secondary (decoupled) chilled water loop configuration, where separate variable speed pumps are dedicated to the primary and secondary water loops. The chillers in the primary water loop, where each chiller has rated cooling capacity from around 1,000 to 1,500 ton, are high-efficiency units with centrifugal compressors and internal capacity controls using variable speed compressor, inlet guide vane and diffuser modulations, and hot-gas bypass for part-load operations. The chiller configuration is a combination of series and parallel connections. Depending on a selection of plant modes, the plant could operate a single chiller, two serially connected chillers, three chillers (two series chillers and one parallel chiller), and four chillers (two parallel chiller groups of chillers where each group has two series chillers). The variable frequency drives for the secondary water pumps adjust the pump speed to regulate the differential pressure between the supply and return pipes to transport the chilled water to multiple building load terminals.

A two million gallon chilled water tank (sensible energy storage) is located at the bypass line (or decoupler) between the primary and secondary water loops. The tank is a stratified cool storage where warmer and less denser water floats on the top of colder and denser water. There are no isolation valves on the bypass line, and therefore the mismatch between primary water flow rate and secondary flow rate determines the charging or discharging flow rate. In order not to disturb the thermocline in the water tank, the chilled water supply temperature setpoint should be maintained at around 39^oF (around 4^oC). This constraint on the chiller leaving temperature together with no-isolation valves on the bypass line results in that the primary water flow rate setpoint as the only decision variable that defines charging and discharging heat rate when chillers are running.

In addition, the UC-Merced campus has more than 4 MW of on-site solar farm which covers 8.5 acres southeast of the campus and an approximately 960-space parking lot. The PV has a single-axis sun tracking system, which captures up to 30% more sunlight than conventional fixed-tilt systems by following the sun throughout the day.

It is important to mention the utility tariff structure which is one of the key driving forces for MPC. Because of the scale of energy consumption, the energy price rate is much more complex than a typical TOU (time of use) structure. It purchases energy from selected energy service providers within the energy wholesale market through a negotiation process. This program makes 1) the time variation of the energy price rate small, and 2) the demand charge is much

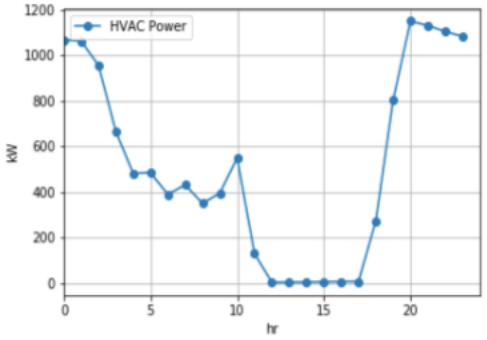

Figure 2: Daily-averaged plant power at the UC-Merced

more dominant than the energy charge at the site.

In this study, the optimization variables to the system are the primary volume flow rate setpoint (V_p) and the plant operation mode (s_j) as depicted in Fig. 1. Note that s_j does not indicate the ON/OFF status of a chiller. Instead, the model activates and deactivates some chiller(s), pumps(s), cooling towers(s) and isolation valve(s), pre-defined by the existing control sequence.

2.2 Description of baseline control

The basic operation strategy for the cooling TES plant is the storage priority control that runs chiller(s) during the nighttime to store cooling energy in the chilled water tank and uses the cooling energy during the day time to fully meet the daytime campus cooling load. Fig. 2 shows a representative plant electrical power profile of the chiller plant operation. To generate this plot, the daily profiles of the total plant electrical power consumption, which aggregates chiller compressor powers, cooling tower fan powers, pump powers for the primary and condensor water pumps, over the month of August were collected and averaged. Note that the plant power is zero from 12:00 to 17:00 hour. This means the chilled water tank completely serves the campus load, which clearly characterizes the control and system as the storage priority control and full storage system. It is important to remember that the storage priority control in general does not account for behind-meter, on-site renewable energy.

3. MIXED INTEGER LINEAR MPC FORMULATION

3.1 Objective function

The control objective for the chiller plant is to minimize utility cost and CO2 emission in the grid region (California Independent System Operator, CAISO), and self-consume the behind meter PV generation.

$$min \sum_{k=0}^{N_p-1} E[k] \times max\{P_{net}[k], 0\} + \omega_d \times d, \tag{1}$$

where E represents a time varying grid signal which could be utility price rate, a carbon emission rate, or a weighted combination of them. P_{net} is the net power consumption of the entire campus measured at the grid connection point which is the total power consumption subtracted by the on-site PV generation, i.e.,

$$P_{net} = P_{plant} + P_{nonplant} - P_{PV}. \tag{2}$$

When P_{net} is positive, the campus imports the power from the grid while the campus exports the power to the grid when negative.

The first term represents time-integrated GHG emission [MTCO2eq], energy cost [$] or a combination of them over the prediction horizon (N_p) depending on the definition of E. Note that we integrate $max\{P_{net}[k], 0\}$ rather than P_{net}. This is to promote the self-consumption of on-site renewable energy by not incentivising power export. ω_d is a weight on the max peak power (d)[1] over the prediction horizon.

[1] Strictly speaking, d is an upper bound of the max peak power over the prediction horizon.

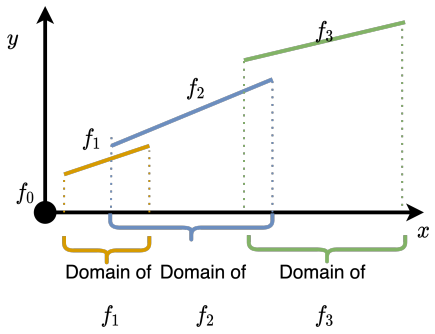

Figure 3: Conceptual plot for a switching system. A feasible set in (x, y)-space switches depending on a mode selection.

3.2 Modeling total plant power as a switching system

Because the plant mode determines a different set of chillers, cooling towers, pumps, and isolation valves, the plant power and COP behaves differently depending on plant modes. Due to this nature, one has to model the total plant power as a switching system regardless of modeling approaches (i.e., white-box, gray-box or black-box models).

We chose the following model structure for the total plant power modeling.

$$P_{plant} = \begin{cases} 0 & \text{for the plant mode 0} \\ a_1 Q_{CH} + b_1(T_{WB}) & \text{for the plant mode 1} \\ \vdots & \\ a_J Q_{CH} + b_J(T_{WB}) & \text{for the plant mode J} \end{cases} \tag{3}$$

where Q_{CH}, T_{WB} are the total chiller load (or the sum of chiller loads), and the outdoor wet-bulb temperature, respectively. a_j is a constant and b_j is a function of T_{WB}, respectively. There is no restriction on the model structure for b_j but the linear affine form, i.e., $b_j = b_{j,0} + b_{j,1} T_{WB}$, is selected in this paper. Since T_{WB} is not an optimization variable, we denote $b_j(T_{WB})$ as b_j for the simplicity of notations.

The technical challenge of a switching system for mathematical programming, in general, is that some constraints appear or disappear depending on a selection of modes because of the IF-THEN nature. For our plant power model of Eqn. (3), the feasible set of (P_{plant}, Q_{CH}) switches via a mode as depicted in Fig. 3. A straightforward approach is to model it as $P_{net} = \sum_j (a_j Q_{CH} + b_j) \times s_j$, but it results in a mixed integer nonlinear programming problem which suffers from the lack of convergence, global optimality (Wolsey, 1998; Elsido et al., 2017), computational efficiency, and MPC closed-loop stability. To resolve this issue, we utilized the Generalized Disjunctive Programming approach as described in the next section.

3.3 Treatment of Switching Plant Power Model using Generalized Disjunctive Programming Approach

3.3.1 Recap of Generalized Disjunctive Programming: The Generalized Disjunctive Programming (GDP) is an alternative mathematical programming approach to the mixed integer programming. It was first introduced by Raman and Grossmann (1994) who extended the Disjunctive Programming (Balas, 1985). Unlike typical programming approaches which only allow algebraic expressions, GDP allows formulating optimization problems with logical expressions. The logical constraints consist of disjunctions and logic propositions. Once an optimization problem is formulated with the logical expressions, GDP provides methods of transforming the disjunctions into mixed-integer (nonlinear/linear) equality and/or inequality constraints, and the logic propositions into integer-only equality and/or inequality constraints. Then, the converted mixed-integer (nonlinear/linear) program is solved by available mixed-integer programming solvers.

There are several representations of a mathematical structure of GDP in the literature, but we introduce the form introduced in (Grossmann and Ruiz, 2012).

$$min\ f(x) + \sum_{k=1}^{K} c_k \quad \text{Objective Function} \tag{4}$$

$$g(x) \le 0 \quad \text{Algebraic Constraints} \tag{5}$$

$$\bigvee_{i \in D_k} \begin{bmatrix} Y_{i,k} \\ A_{i,k}x_k \le b_{ik} \\ c_k = \gamma_{ik} \end{bmatrix} \quad \text{Disjunctions} \tag{6}$$

$$\Omega(Y) = True \quad \text{Propositions} \tag{7}$$

$$L \le x \le U, x \in \mathbb{R}^n, c_k \in \mathbb{R}^1 \quad \text{Continuous Variables} \tag{8}$$

$$Y_{i,k} \in \{True, False\} \quad \text{Boolean Variables} \tag{9}$$

- $f\,(:\mathbb{R}^n \to \mathbb{R}^1), g\,(:\mathbb{R}^n \to \mathbb{R}^m)$ are a function and algebraic constraints of continuous variables x
- K represents the number of disjunctions
- Y_{ik} is a Boolean variable that controls the feasible space where the global continuous variable, x, lies (represented by the inequality constraint) and the cost represented by the equality constraint in Eqn. (6). That is, when $Y_{i,k} = True$, the constraints of $A_{i,k}x_k \le b_{ik}, c_k = \gamma_{ik}$ apply. Otherwise, they are ignored.
- D_k is a set of integers associated with the k-disjunction
- Ω is a propositional logic involving only the Boolean variables

Note Y_{ik} is controls the feasible space depending on the value of Y_{ik}. This is exactly the problem for a switching system discussed in Section 3.2.

The conversion of the above disjunctions and logic propositions to algebraic expressions can be done systematically by utilizing either the Big-M method or the Convex-Hull approach. The latter approach finds the convex hull (that is the minimal convex envelope) of the disjunctive sets, and hence provides a tighter convex envelope than that of the Big-M approach. In addition, it does not require tuning parameters as opposed to the Big-M method. The Convex-Hull approach leads to the following mixed-integer program.

$$min\ f(x) + \sum_{k=1}^{K} c_k \tag{10}$$

$$g(x) \le 0 \tag{11}$$

$$\sum_{i \in D_k} y_{i,k} = 1 \qquad k \in \{1, \cdots, K\} \tag{12}$$

$$A_{i,k}v_{i,k} \le b_{i,k}y_{i,k} \quad k \in \{1, \cdots, K\}, i \in D_k \tag{13}$$

$$x_k = \sum_{i \in D_k} v_{i,k} \qquad k \in \{1, \cdots, K\} \tag{14}$$

$$c_k = \sum_{i \in D_k} \gamma_{i,k}y_{i,k} \qquad k \in \{1, \cdots, K\} \tag{15}$$

$$0 \le v_{i,k} \le U_v y_{i,k} \quad k \in \{1, \cdots, K\}, i \in D_k \tag{16}$$

$$Ay \ge a \tag{17}$$

$$L \le x \le U, x \in \mathbb{R}^n, c_k \in \mathbb{R}^1 \tag{18}$$

$$y_{i,k} \in \{0, 1\} \tag{19}$$

where $y_{i,k}$ is the binary variable that corresponds to $Y_{i,k}$, $v_{i,k}$ is an axially variable and U_v is an upper bound for $v_{i,k}$. Please refer to Grossmann and Ruiz (2012) for detailed discussions.

3.3.2 Application of Generalized Disjunctive Programming: According to the GDP modeling approach, Eqn. (3) can be expressed as follows.

$$\begin{bmatrix} S_0 \\ Q_{CH} = 0 \\ P_{plant} = 0 \end{bmatrix} \quad \vee \quad \begin{bmatrix} S_1 \\ Q_{min,1} \le Q_{CH} \le Q_{max,1} \\ P_{plant} = a_1 Q_{CH} + b_1 \end{bmatrix} \vee \cdots \vee \begin{bmatrix} S_J \\ Q_{min,J} \le Q_{CH} \le Q_{max,J} \\ P_{plant} = a_J Q_{CH} + b_J \end{bmatrix}, \tag{20}$$

where S_j is the Boolean variable indicating an active plant mode. That is, when $S_j = True$, the j^{th} constraints become active, and vice versa.

Applying the Convex-Hull approach and eliminating the redundancy associated with the 0^{th} mode result in the following desired, mixed-integer constraints.

$$\sum_{j=1}^{J} s_j \le 1 \tag{21}$$

$$s_j Q_{min,j} \le v_j \le Q_{max,j} s_j, \quad j \in \{1, \cdots, J\} \tag{22}$$

$$\mu_j = a_j v_j + b_j s_j, \quad j \in \{1, \cdots, J\} \tag{23}$$

$$Q_{CH} = \sum_{j=1}^{J} v_j \tag{24}$$

$$P_{plant} = \sum_{j=1}^{J} \mu_j \tag{25}$$

where $v_1, \cdots, v_J$ are the auxiliary variables for Q_{CH}, and $\mu_1, \cdots, \mu_J$ are the auxiliary variables for P_{plant}.

Note that, when any k ($\in \{1, \cdots, J\}$) is selected, then $s_{j,j\neq k} = 0$ and $v_{j,j\neq k} = 0$ from Eqns. (22) and (23), and therefore $Q_{CH} = v_k$, $Q_{min,k} \le v_k \le Q_{max,k}$, and $P_{plant} = a_k Q_{CH} + b_k$ which are the desired algebraic constraints. When none of modes is selected, i.e., $s_1 = 0, \cdots, s_J = 0$, $Q_{CH} = 0, P_{plant} = 0$. Note also that all equality and inequality constraints are linear in v_j, μ_j, s_j, Q_{CH} and P_{plant}.

3.4 Start-up and shut-down constraint

It is well known that frequent mode switching causes negative impacts on the life of equipment and part-load performance. An intuitive approach is to add a penalty whenever the mode changes. However, it was not trivial to tune the weights, and it is not applicable to our case since one has to shut down the chiller whenever the storage is fully charged for example. To resolve this, we adopted the mathematical programming approach from the Unit Commitment problem (Rajan et al., 2005; Knueven et al., 2020) in the electrical power system. This method enforces minimal ON or OFF times for each unit operation: that is, once a power generation unit is activated (deactivated), it has to maintain the ON (OFF) status at least for a predefined minimal ON (OFF) time period. Application to our system is described as follows.

For the j^{th} mode and a time-step k, let $\delta_{ON,j}[k]$ ($\in \{0, 1\}$) and $\delta_{OFF,j}[k]$ ($\in \{0, 1\}$) be turn-ON and turn-OFF variables, respectively. The relationship between those variables is

$$s_j[k] - s_{j-1}[k] = \delta_{ON,j}[k] - \delta_{OFF,j}[k] \ (k \in \{0, \cdots, N_p - 1\}, j \in \{1, \cdots, J\}). \tag{26}$$

In addition, we impose the following constraint to prevent the situation where turning ON and OFF occur simultaneously.

$$\delta_{ON,j}[k] + \delta_{OFF,j}[k] \le 1 \tag{27}$$

Let OT_j be the minimal run-time for the j mode. The formulations to incorporate the minimal run-time in the MPC formulation are as follows.

1) For $k \geq OT_j - 1$,

$$\sum_{l=0}^{OT_j-1} \delta_{ON,j}[k-l] \leq s_j[k] \tag{28}$$

$$\sum_{l=0}^{OT_j-1} \delta_{OFF,j}[k-l] \leq 1 - s_j[k]. \tag{29}$$

2) For $k < OT_j - 1$,

$$\sum_{l=1}^{OT_j-k-1} \delta_{ON,j}^{history}[-l] + \sum_{l=0}^{k} \delta_{ON,j}[k-l] \leq s_j[k] \tag{30}$$

$$\sum_{l=0}^{OT_j-k-1} \delta_{OFF,j}^{history}[-l] + \sum_{l=0}^{k} \delta_{OFF,j}[k-l] \leq 1 - s_j[k]. \tag{31}$$

3.5 Reformulation of the objective function

Remember that we tend not to incentivize the negative net power by using the max function in Eqn. (1) in order to promote the self-consumption of the on-site PV. Technically, the term $\sum_{k=0}^{N_p-1} E[k] \times max\{P_{net}[k], 0\}$ constitutes a mixed integer convex program. It would be greatly useful to have an equivalent mixed integer linear program, if possible, for the use of fast and reliable solvers (e.g., CPLEX, GLPK, Gurobi, LPSOLVE) and for better scalability to the increase of the number of variables.

Like the epi-graph formulation (Boyd et al., 2004), we may define an upper bound of $max\{P_{net}[k], 0\}$ for each k, put inequality constraints to replace each max term with the upper bound, and minimize the upper bounds. This approach was strictly proved (the proof is not omitted in this paper due to the page limit). The conclusive, mixed integer linear formulation for Eqn. (1) is;

$$min \qquad \sum_{k=0}^{N_p-1} \left(E[k] \times P_{net}^{+}[k] \right) + \omega_d \times d \tag{32}$$

$$P_{plant}[k] + P_{nonplant}[k] - P_{PV}[k] \leq P_{net}^{+}[k] \ (k \in \{0, \cdots, N_p - 1\}) \tag{33}$$

$$0 \leq P_{net}^{+} \ (k \in \{0, \cdots, N_p - 1\}) \tag{34}$$

where $P_{net}^{+}[\cdot]$ are auxiliary variables.

4. SITE PERFORMANCE OF MPC

The presented MPC has been implemented for the campus cooling TES plant for several test periods, and sample test results for a week in May 2021 are shown and discussed in this section. We start describing our approach to evaluate performance of MPC compared with the baseline control described in Section 2.2.

4.1 Selection of baseline control period for actual performance assessment

To make fair comparisons between two controllers and evaluate actual performance for the real site, a baseline period was carefully selected considering the followings: 1) the baseline control was implemented, 2) uncontrollable disturbances including campus cooling load, MOER signal and on-site solar generation were consistent to that of the MPC period, and 3) initial and final SOC were close enough.

4.2 MPC performance assessment

4.2.1 Comparisons of closed-loop responses between baseline control and MPC: Fig. 4 compares the closed-loop responses of the baseline control and the MPC. The first sub-figure shows the campus net power consumptions, i.e., total consumption subtracted by the on-site PV generation, and the second sub-figure shows the profiles of the state of charge (measured from the relative height of the thermocline) for the two control periods. The blue and red colors are dedicated to the baseline control and MPC, respectively. The shaded areas indicate when the MOER is higher than 0.3 [mTonCO2e/MWh] that is equal to the average level of GHG emission for a natural gas power plant in the U.S. according to the EPA's Emissions and Generation Resource Integrated Database (eGRID). In other words, the shaded

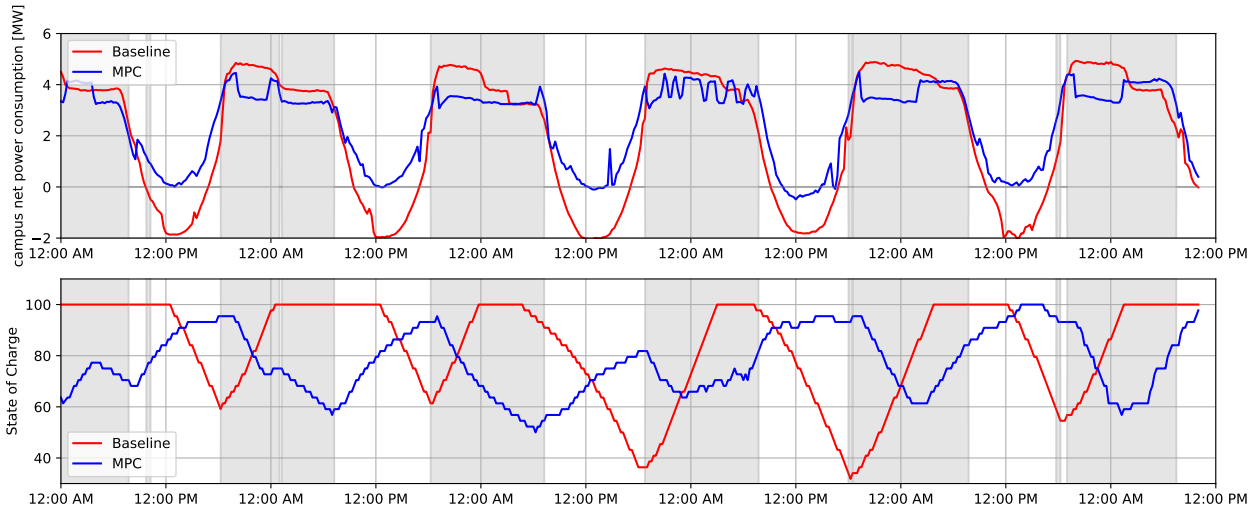

Figure 4: Comparisons of experimental net power consumption and state of charge between the baseline and MPC at UC-Merced (red: baseline, blue: MPC)

areas are when the grid is dirty, and non-shaded areas are when the grid is clean. First, look at the afternoon period for the first day where the state of the charge decreases from 100% to 60% for the baseline control. This means that the control utilizes the stored thermal energy to meet the entire campus cooling load during the daytime period. For the time being, the chillers were off, causing significant excessive power around 2 MW that was sent back to the grid as shown in the first subfigure. Compare the behavior of the state of charge with the MPC for the same period. The MPC actually increased the state of the charge which implies that the chillers were ON, met the entire campus cooling load and charged the storage. Since the MPC increased the chiller power during the period, the excessive power export was eliminated as shown in the first subfigure. Second, when the grid condition got dirtier, the baseline control increased the state of charge and this charging process continued until the TES was fully charged (see the evening time for the first day in the second subfigure). On the other hand, the MPC consumed less energy when the grid was dirty by leveraging the stored energy from the on-site renewable. This pattern repeats for the entire test period as shown in the figure.

It should be mentioned that facility operators requested to preserve 50% to 60% of the charge level during the MPC implementation period which significantly limits savings potentials. This can be confirmed in the second subfigure.

The baseline control which is independent of renewable consumed 23.7 MWh (daily average) out of 32.6 MWh (daily average) total solar generation, resulting in 72.8% self-consumption ratio. On the other hand, the MPC control consumed almost all on-site PV energy resulting in a 99.2% self-consumption ratio. In other words, the increment of the self-consumption ratio via MPC is 26.4%.

The comparison of GHG emission rates are shown in Fig. 5. One can see visible reduction in the emission rate. The daily average value of the carbon reductions using the MPC is 1 [mTonCO2e] per day. The unit metric ton CO2e is equivalent to the emission rate driving a car for around 2,500 miles or 4,023 km (roughly San Francisco, California to Washington, DC). Again, the reduction was achieved by coordinating operations of cooling TES plant with on-site PVs in response to the grid carbon emission signal. The calculated GHG savings is around 10% but it is anticipated that more than 20% reduction can be achievable for the plant once the minimum state of charge constraint (varied between 50% to 60%) can be relaxed.

The peak power reduction was around 10%. It is not that significant considering the size of the tank (2 million gallons of water). This is mainly because the facility operators requested to preserve 50% to 60% of the charge level during the MPC implementation period. This significantly limits the capability of a peak demand reduction and CO2 reduction,

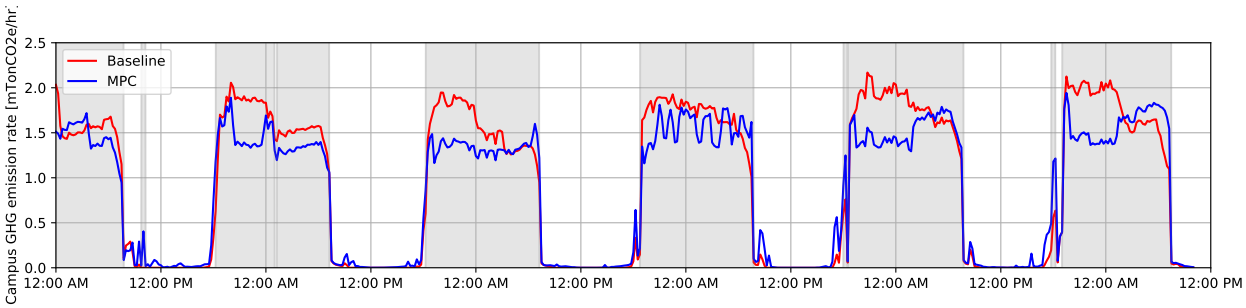

Figure 5: Comparisons of GHG emission rate between MPC and baseline storage-priority control at the UC-Merced

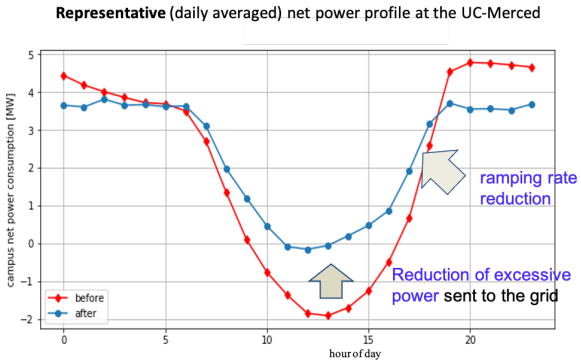

Figure 6: Comparisons of representative (daily averaged) net power profiles between the baseline control and MPC at the UC-Merced for the weeks of evaluation in May

because during the nighttime chillers have to run to maintain the minimum charge level. If the strong constraint has been relaxed, MPC would not need to operate chillers for the nighttime and would increase the savings. It should be mentioned that even with the conservative 10% peak reduction, it attracts the interest of facility operators because of the magnitude of power consumption for the campus-level cooling plant. For the UC-Merced case, the utility cost savings are around ten thousand dollars per month.

4.2.2 Benefits of MPC to the grid: Although the time series comparison provides comprehensive information, it is difficult to capture the overall behavior of the MPC. To more clearly characterize this behavior, we averaged daily power consumption profiles for the two controls and they are shown in Fig. 6. Like before, the blue and red lines are associated with the baseline control and MPC. It is interesting to see that the representative (daily averaged) profiles at the site look similar to the duck-curve which the grid is experiencing. This figure clearly shows that the MPC consumes and stores more energy during the daytime using the clean on-site solar, and consumes less during evening and night time when the grid gets dirty by leveraging the stored energy.

The smooth load curve could provide significant benefits to the grid, because 1) The higher consumption during the daytime addresses the issue of high renewable curtailment in CAISO, 2) The proper operation of the chilled water storage in response to the on-site renewable allows tolerating the increasing PV penetration to the grid, 3) The reduced ramping rate during the evening time addresses the issue of running gas turbines to follow the high ramping rate of the neck of the duck-curve as discussed in Introduction, and 4) The self-consumption of the behind-meter solar reduces the concern of voltage regulation in the distribution line and improves the grid reliability and efficiency.

5. CONCLUSIONS

Cooling TES plants are one of the oldest and reliable energy storage technologies. This paper shows that cooling plants with existing TES could be one of the most cost-effective resources to achieve state and government' carbon neutrality goals, since it does not require installing new energy storage but only requires changing the operation. We

presented a novel, Generalized Disjunctive Programming-based MPC and its site performance for a campus-level cooling TES plant that coordinates operations of multiple chillers, chilled water tank and behind-meter PVs. It aims at self-consuming on-site 4 MW solar farms, lowering carbon emission at the grid and minimizing utility bills. The performance of MPC was assessed by comparing with a carefully selected baseline period where the storage priority control has been implemented. The MPC reduced the excess PV power by around 25%, the greenhouse gas emission by 10%, and peak demand by 10%. The savings estimates were conservative, since only a partial usage of the chilled water tank was allowed during the MPC implementation period. The capability of achieving utility peak demand in addition to lowering GHG emission is the uniqueness of the MPC. Future work will include a longer-term implementation of the MPC (> 1 year) to provide a more comprehensive savings assessment and reliability of the MPC technology.

REFERENCES

Balas, E. (1985). Disjunctive programming and a hierarchy of relaxations for discrete optimization problems. *SIAM Journal on Algebraic Discrete Methods*, 6(3):466–486.

Boyd, S., Boyd, S. P., and Vandenberghe, L. (2004). *Convex optimization*. Cambridge university press.

Elsido, C., Bischi, A., Silva, P., and Martelli, E. (2017). Two-stage minlp algorithm for the optimal synthesis and design of networks of chp units. *Energy*, 121:403–426.

Grossmann, I. E. and Ruiz, J. P. (2012). Generalized disjunctive programming: A framework for formulation and alternative algorithms for minlp optimization. In *Mixed Integer Nonlinear Programming*, pages 93–115. Springer.

Knueven, B., Ostrowski, J., and Watson, J.-P. (2020). A novel matching formulation for startup costs in unit commitment. *Mathematical Programming Computation*, 12(2):225–248.

Rajan, D., Takriti, S., et al. (2005). Minimum up/down polytopes of the unit commitment problem with start-up costs. *IBM Res. Rep*, 23628:1–14.

Raman, R. and Grossmann, I. E. (1994). Modelling and computational techniques for logic based integer programming. *Computers & Chemical Engineering*, 18(7):563–578.

Tarragona, J., Pisello, A. L., Fernández, C., de Gracia, A., and Cabeza, L. F. (2021). Systematic review on model predictive control strategies applied to active thermal energy storage systems. *Renewable and Sustainable Energy Reviews*, 149:111385.

Wolsey, L. A. (1998). Integer programming john wiley & sons. *New York, NY*, 4.

ACKNOWLEDGEMENT

This work was supported by the Assistant Secretary for Energy Efficiency and Renewable Energy, Building Technologies Office and the U.S. China Clean Energy Research Center, Building Energy Efficiency (CERC-BEE) program, of the U.S. Department of Energy under Contract No. DE-AC02-05CH11231. The authors would like to thank Tim Olson, Michael Pearson, Robert Stefanski, Danny Ward, Francisco Cazares-Moreno, Eric Cardoza and Victor Zaragoza from University California, Merced for their strong support for this site demonstration work. Special thanks to James Brugger and Michael Logsdon for constructive feedback and technical support, and to Erika Gupta from Building Technologies Office of U.S. Department of Energy for her support on the project.